

Valley separation in graphene by polarized light

L. E. Golub and S. A. Tarasenko

Ioffe Physical-Technical Institute of the RAS, 194021 St. Petersburg, Russia

M. V. Entin⁽¹⁾ and L. I. Magarill^(1,2)

⁽¹⁾ *Institute of Semiconductor Physics, Siberian Branch of the RAS, 630090 Novosibirsk, Russia*

⁽²⁾ *Novosibirsk State University, 630090 Novosibirsk, Russia*

We show that the optical excitation of graphene with polarized light leads to the pure valley current where carriers in the valleys counterflow. The current in each valley originates from asymmetry of optical transitions and electron scattering by impurities owing to the warping of electron energy spectrum. The valley current has strong polarization dependence, its direction is opposite for normally incident beams of orthogonal linear polarizations. In undoped graphene on a substrate with high susceptibility, electron-electron scattering leads to an additional contribution to the valley current that can dominate.

PACS numbers: 78.67.Wj, 72.80.Vp, 73.50.Pz

Graphene, one-atom-thick layer of carbon with the honeycomb crystal lattice, has been attracting rapidly growing attention due to its unique electronic properties. Zero band gap and zero effective electron and hole masses as well as high enough mobility make it perspective for fundamental and applied research.^{1–3} The electron excitations in graphene are similar to massless Dirac fermions with the cone points situated at the points K and K' of the Brillouin zone. The interplay of two equivalent valleys gives rise to new transport and optical phenomena, which are absent in systems with simple electron dispersion, and underlies the novel research field called “valleytronics”.^{4,5} In multivalley structures, one can independently control the carriers in different valleys and construct peculiar electron distribution where particles in the valleys flow predominantly in different directions.⁶

Previous research of valley-dependent transport in graphene was focused on the manipulation of charge carriers by static electric field. It was demonstrated that the electric field may induce valley-polarized current in a graphene point contact with zigzag edges,⁵ graphene layer with broken inversion symmetry,⁷ bilayer graphene,⁸ or if the structure is additionally illuminated by circularly polarized radiation.⁹ It was also proposed in Ref. [10] that valley currents can be induced in mesoscopic graphene rings by asymmetrical monocycle electromagnetic pulses. Here, we show that the valley separation can be achieved in a homogeneous graphene layer by pure optical means. We demonstrate that the interband excitation of graphene by linearly polarized light leads to the electron current in each valley, which direction is determined by the light polarization. The partial photocurrents $j^{(\nu)}$ ($\nu = \pm$ for the valleys K and K' , respectively) in the ideal honeycomb structure are directed oppositely, so that the total electric current $j^{(+)} + j^{(-)}$ vanishes. We also briefly discuss optical and transport methods to reveal the pure valley current.

Phenomenologically, the emergence of the valley photocurrent is related to the low point-group symmetry of individual valleys. Despite the fact that the crystal lat-

tice of flat graphene is centrosymmetric, the valleys K and K' are described by the wave vector group D_{3h} lacking the space inversion, see Fig. 1. The group D_{3h} allows for the photocurrent induced by normally-incident linearly polarized light. The polarization dependences of the current components in the valley K are given by

$$j_x^{(+)} = \chi(e_x^2 - e_y^2)I, \quad j_y^{(+)} = -2\chi e_x e_y I. \quad (1)$$

Here, χ is a parameter, e_x and e_y are components of the (real) light polarization unit vector \mathbf{e} , I is the intensity of incident light, and the x axis is chosen along the Γ - K line, Fig. 1a. The photocurrent in the valley K' is obtained from Eq. (1) by the replacement $x \rightarrow -x$, which gives $j^{(-)} = -j^{(+)}$. We note that the absence of a total electric current at normal incidence of radiation is in agreement with the symmetry arguments allowing for a photocurrent in noncentrosymmetric systems only. At oblique incidence of the radiation, a net current in graphene may arise due to the photon drag effect.^{11,12}

The microscopic model of pure valley current generation is based on the trigonal warping of energy spectrum

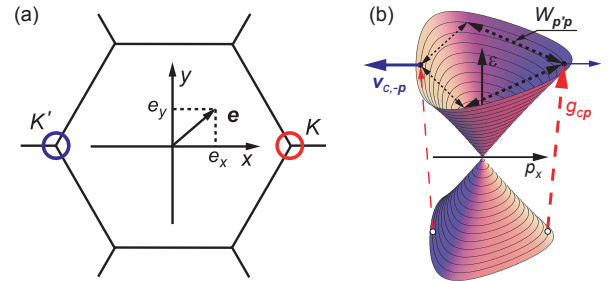


FIG. 1: (color online) (a) Brillouin zone of graphene. The circles indicate neighborhood of the K and K' points where the electron states have trigonal symmetry allowing for the photocurrent. (b) Mechanisms of photocurrent formation in the K valley. Solid, dashed, and dotted arrows of different thicknesses indicate anisotropy of velocity, optical generation, and scattering rate, respectively, in \mathbf{p} -space.

of carriers in the valleys. The effective Hamiltonian describing electron and hole states in the vicinity of the K and K' points has the form¹³

$$\hat{H}_{\mathbf{p}}^{(\nu)} = \begin{pmatrix} 0 & \Omega_{\mathbf{p}}^{(\nu)} \\ \Omega_{\mathbf{p}}^{(\nu)*} & 0 \end{pmatrix}. \quad (2)$$

Here, \mathbf{p} is the momentum counted from the valley center,

$$\Omega_{\mathbf{p}}^{(\nu)} = \nu v_0(p_x - ip_y) - \mu(p_x + ip_y)^2, \quad (3)$$

v_0 is the electron velocity, and μ is the parameter of warping that reflects the trigonal symmetry of valleys (D_{3h} wave vector group). In the framework of tight-binding model, $\mu = v_0 a / (4\sqrt{3}\hbar)$ with a being the lattice constant.² We assume that the warping is small and, therefore, calculate the current to first order in μ . The energy spectrum of carriers in the conduction (c) and valence (v) bands is given by

$$\varepsilon_{c\mathbf{p}}^{(\nu)} \approx v_0 p - \nu \mu p^2 \cos 3\varphi_{\mathbf{p}}, \quad \varepsilon_{v\mathbf{p}}^{(\nu)} = -\varepsilon_{c\mathbf{p}}^{(\nu)}, \quad (4)$$

where $\varphi_{\mathbf{p}}$ is the polar angle of the momentum \mathbf{p} .

Shown in Fig. 1b is the energy spectrum in the K valley with the warping being included. The inequality of $\varepsilon_{c\mathbf{p}}^{(+)}$ and $\varepsilon_{c,-\mathbf{p}}^{(+)}$ (as well as $\varepsilon_{v\mathbf{p}}^{(+)}$ and $\varepsilon_{v,-\mathbf{p}}^{(+)}$) gives rise to an electric current in the valley if electrons are optically excited from the valence to conduction band by linearly polarized light. In the valley K' , the warping of energy spectrum is opposite, Eq. (4), and the photocurrent direction is reversed.

In the framework of kinetic theory, the photocurrent densities in the valleys are given by

$$\mathbf{j}^{(\nu)} = 2e \sum_{\mathbf{p}} \left(\mathbf{v}_{c\mathbf{p}}^{(\nu)} f_{c\mathbf{p}}^{(\nu)} + \mathbf{v}_{v\mathbf{p}}^{(\nu)} f_{v\mathbf{p}}^{(\nu)} \right), \quad (5)$$

where e is the electron charge, the factor 2 accounts for spin degeneracy, $\mathbf{v}_{c,v}^{(\nu)} = \nabla_{\mathbf{p}} \varepsilon_{c,v}^{(\nu)}$ are the velocities, and $f_{c\mathbf{p}}^{(\nu)}$ and $f_{v\mathbf{p}}^{(\nu)}$ are the nonequilibrium corrections to the distribution functions in the conduction and valence bands linear in the light intensity; $f_{c\mathbf{p}}^{(+)} = f_{c,-\mathbf{p}}^{(-)}$ and $f_{v\mathbf{p}}^{(+)} = f_{v,-\mathbf{p}}^{(-)}$ due to space inversion symmetry. We consider interband optical transitions in undoped graphene at low temperature. Owing to electron-hole symmetry $f_{c\mathbf{p}}^{(\nu)} = -f_{v\mathbf{p}}^{(\nu)}$, and the photocurrent Eq. (5) assumes the form $\mathbf{j}^{(\nu)} = 4e \sum_{\mathbf{p}} \mathbf{v}_{c\mathbf{p}}^{(\nu)} f_{c\mathbf{p}}^{(\nu)}$.

The steady-state correction to the distribution function can be found from the kinetic equation

$$\sum_{\mathbf{p}'} \left(W_{\mathbf{p}\mathbf{p}'}^{(\nu)} f_{c\mathbf{p}'}^{(\nu)} - W_{\mathbf{p}'\mathbf{p}}^{(\nu)} f_{c\mathbf{p}}^{(\nu)} \right) + \text{St}^{(\text{ee})} + g_{c\mathbf{p}}^{(\nu)} = 0, \quad (6)$$

where $W_{\mathbf{p}\mathbf{p}'}^{(\nu)}$ is the rate of intravalley electron scattering by static defects or impurities, the weak intervalley processes are neglected, $g_{c\mathbf{p}}^{(\nu)}$ is the optical generation rate, and $\text{St}^{(\text{ee})}$ describes electron-electron collisions.

First, we consider the valley current in the presence of intensive electron scattering by impurities and neglect electron-electron collisions. We focus on the photocurrent in the K valley and omit index $\nu = +$. In the Born approximation, the rate of elastic electron scattering by impurities $W_{\mathbf{p}\mathbf{p}'} = W_{\mathbf{p}'\mathbf{p}}$ is given by

$$W_{\mathbf{p}\mathbf{p}'} = \frac{\pi}{2\hbar} \left| 1 + \frac{\Omega_{\mathbf{p}} \Omega_{\mathbf{p}'}^*}{|\Omega_{\mathbf{p}} \Omega_{\mathbf{p}'}|} \right|^2 \mathcal{K}(|\mathbf{p}' - \mathbf{p}|) \delta(\varepsilon_{c\mathbf{p}} - \varepsilon_{c\mathbf{p}'}), \quad (7)$$

where $\mathcal{K}(q)$ is the Fourier component of the impurity potential correlator. The specific angular dependence of $W_{\mathbf{p}\mathbf{p}'}$ follows from the Hamiltonian Eq. (2). The generation rate in the conduction band $g_{c\mathbf{p}}$ is determined by the interband matrix elements of the velocity operator $\nabla_{\mathbf{p}} \hat{H}_{\mathbf{p}}$ and has the form

$$g_{c\mathbf{p}} = \frac{2\pi}{\hbar} \left(\frac{eA}{c} \right)^2 \left| \text{Im} \left(\frac{\Omega_{\mathbf{p}}^*}{|\Omega_{\mathbf{p}}|} \mathbf{e} \cdot \nabla_{\mathbf{p}} \Omega_{\mathbf{p}} \right) \right|^2 \delta(\hbar\omega - 2\varepsilon_{c\mathbf{p}}). \quad (8)$$

Here ω is the light frequency, $A/2$ is the amplitude of the vector potential of the electromagnetic wave related to the intensity of incident light by $I = A^2 \omega^2 / (2\pi c t_0^2)$, and t_0 is the amplitude transmission coefficient, $t_0 = 2/(n+1)$ for graphene on a substrate with the refractive index n .

As follows from Eqs. (5) and (6), the valley current arises owing to warping-induced asymmetry in the electron velocity $\mathbf{v}_{c\mathbf{p}}$, the scattering rate $W_{\mathbf{p}\mathbf{p}'}$, and the generation rate $g_{c\mathbf{p}}$. Accordingly, to first order in μ one can distinguish three contributions to the current Eq. (1), $\chi = \chi^{(\text{vel})} + \chi^{(\text{gen})} + \chi^{(\text{sc})}$. The corresponding mechanisms of the current formation are sketched in Fig. 1b.

To calculate the valley current caused by the velocity correction one neglects the warping in optical generation and scattering rates. In this mechanism, the absorption of linearly polarized light leads to the alignment of electron momenta described by the second angular harmonic of the distribution function.¹⁴ Owing to the μ -linear correction to the velocity, such a distribution of carriers in \mathbf{p} -space implies an electric current Eq. (1) with

$$\chi^{(\text{vel})} = \frac{5e\mu\eta\tau_2(\varepsilon_{\omega})t_0^2}{8v_0}. \quad (9)$$

Here, $\varepsilon_{\omega} = \hbar\omega/2$ is the kinetic energy of photoelectrons, τ_n ($n = 1, 2, \dots$) are the relaxation times of the n th angular harmonics of the distribution function, $\tau_n^{-1} = \sum_{\mathbf{p}'} W_{\mathbf{p}\mathbf{p}'} (1 - \cos n\theta)$, θ is the angle between \mathbf{p} and \mathbf{p}' , and $\eta = \pi e^2 / \hbar c$ is the absorbance (Ref. [3]) for normally-incident light.

Another contribution to the valley current comes from the asymmetry of photoexcitation. Indeed, to first order in μ , the optical generation rate $g_{c\mathbf{p}}$ contains the first angular harmonic, which gives rise to a photocurrent

$$\chi^{(\text{gen})} = -\frac{e\mu\eta t_0^2}{8v_0} \left[9\tau_1(\varepsilon_{\omega}) + \varepsilon_{\omega} \frac{d\tau_1(\varepsilon_{\omega})}{d\varepsilon_{\omega}} \right]. \quad (10)$$

The third mechanism of the current generation originates from the asymmetry of electron scattering. The

solution of kinetic Eq. (6), $f_{c\mathbf{p}}$, contains the first angular harmonic even if the warping is neglected in the optical generation rate. Such a contribution to the valley current is given by

$$\chi^{(sc)} = \frac{e\mu\eta\tau_2 t_0^2}{8v_0} \left\{ 20 - 6\frac{\tau_1}{\tau_2} - 4\frac{\tau_1}{\tau_3} + \frac{\varepsilon_\omega}{2} \left[\left(\frac{9}{\tau_1} - \frac{2}{\tau_2} \right) \frac{d\tau_1}{d\varepsilon_\omega} + \tau_1 \frac{d}{d\varepsilon_\omega} \left(\frac{1}{\tau_2} + \frac{1}{\tau_3} \right) \right] \right\}, \quad (11)$$

where the relaxation times are taken at the energy ε_ω .

Equations (9)-(11) demonstrate that both the magnitude and excitation spectrum of the pure valley current are determined by the mechanisms of scattering. For electron scattering by unscreened Coulomb impurities in graphene, one obtains $\tau_1 \propto \varepsilon$, $\tau_2 = 3\tau_1$, and $\tau_3 = 5\tau_1$. Such relations yield $\chi \propto \omega$. In the case of scattering by short-range static defects, one has $\tau_1 \propto 1/\varepsilon$, $\tau_2 = \tau_3 = \tau_1/2$ and, therefore, $\chi \propto 1/\omega$. Estimation shows that the valley currents in suspended graphene $j^{(\pm)} \sim 10^{-4}$ A/cm at the light intensity $I = 1$ W/cm², $\tau_1 = 10^{-12}$ s, $\mu = 3.6 \times 10^{26}$ g⁻¹, and $v_0 = 10^8$ cm/s.

Now, we analyze the effect of electron-electron interaction on the pure valley current. It is well known that, in systems with parabolic energy spectrum, the interparticle collisions partially suppress the anisotropy of the distribution function. Therefore, one can expect that electron-electron scattering (between carriers from the same valley and, in particular, between carriers from different valleys) can only decrease the pure valley current. We demonstrate below that the interparticle collisions in graphene may give rise to an additional contribution to the valley photocurrent.

Consider the collision of a photoelectron with the momentum \mathbf{p} from the valley ν of the conduction band with an electron with the momentum \mathbf{k} from the valley ν' of the valence band. After the collision, both electrons occur in the conduction band with the momenta \mathbf{p}' and \mathbf{k}' , respectively, see the left inset in Fig. 2. Processes of other kinds are negligible in undoped graphene at low temperature and weak excitation level. The Coulomb interaction between carriers leads to the transfer of momentum $q \sim \omega/v_0 \ll \pi/a$, therefore, both electrons remain in the valleys they were before the collision although the valleys ν and ν' may be different. The momentum and energy conservation laws read

$$\mathbf{p} + \mathbf{k} = \mathbf{p}' + \mathbf{k}', \quad \varepsilon_{c\mathbf{p}}^{(\nu)} + \varepsilon_{v\mathbf{k}}^{(\nu')} = \varepsilon_{c\mathbf{p}'}^{(\nu)} + \varepsilon_{c\mathbf{k}'}^{(\nu')}. \quad (12)$$

In the conic approximation, Eqs. (12) imply that $k < p$, $p' + k' < p$, and \mathbf{k} should be antiparallel while \mathbf{p}' and \mathbf{k}' parallel to \mathbf{p} .¹⁵ The possibility of the collisions is determined by corrections to the linear dispersion. Interaction-induced renormalization of the energy spectrum makes it concave,^{16,17} which forbids such Auger-like processes. On the contrary, the spectrum warping does allow for the processes. In graphene on a substrate with high susceptibility, the interaction effects are

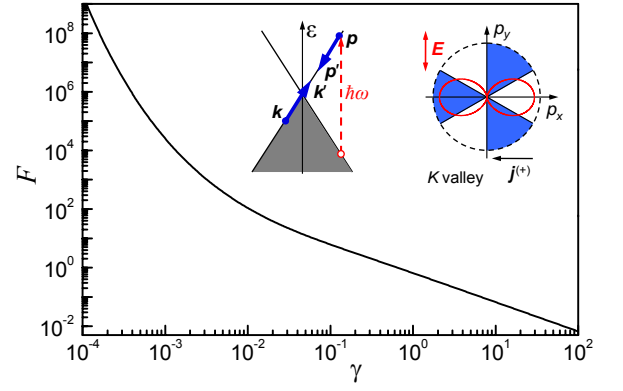


FIG. 2: (color online) Dependence $F(\gamma)$ that determines the magnitude of valley current caused by electron-electron scattering, Eq. (17). Left inset sketches scattering of electrons with the momenta \mathbf{p} and \mathbf{k} into the states with momenta \mathbf{p}' and \mathbf{k}' . Right inset shows the momentum space in the K valley. Sectors where the Auger-like electron relaxation is allowed are colored, ellipses depict the alignment of photoelectron momenta by linearly polarized light.

suppressed and the warping becomes prevailing. An estimation shows that, for an electron with the energy $\varepsilon = 0.3$ eV, this regime occurs at the effective dielectric constant $\varepsilon^* > 300$. Besides, interaction effects can be suppressed by a metallic gate or increasing the temperature. Neglecting the interaction-induced renormalization of the energy spectrum, we obtain from Eqs. (12) to first order in μ

$$v_0 (pk\alpha^2 + p'k'\beta^2) = -2\mu\nu(p - p')(p' + k')[p + p' + \nu\nu'(k - k')] \cos 3\varphi_{\mathbf{p}}, \quad (13)$$

where $\alpha = \varphi_{\mathbf{p}} - \pi - \varphi_{\mathbf{k}} \ll 1$ and $\beta = \varphi_{\mathbf{k}'} - \varphi_{\mathbf{p}'} \ll 1$. Equation (13) has solutions only for sectors of $\varphi_{\mathbf{p}}$ where the second line is positive, i.e., for $\mu\nu \cos 3\varphi_{\mathbf{p}} < 0$. It means that Auger-like processes for electrons with the momentum \mathbf{p} are allowed or forbidden depending on the sign of $\cos 3\varphi_{\mathbf{p}}$, see the right inset in Fig. 2.

The angular dependence of the electron-electron collision rate in graphene gives rise to a pure valley current if the sample is illuminated by linearly polarized light. The mechanism of the current generation is sketched in the right inset in Fig. 2. The absorption of linearly polarized light leads to the alignment of electron momenta described by the second angular harmonic of the distribution function. The photoexcited electrons are scattered by resident electrons from the valence band and lose their energies. Since the scattering rate is anisotropic, the energy relaxation leads to the formation of first harmonic of the distribution function and to an electric current if the momentum relaxation time depends on energy. In the case of weak electron-electron scattering, $\tau_{ee} \gg \tau_1$, where τ_{ee} is the electron-electron scattering time, the mechanism efficiency can be estimated as $\chi^{(ee)} \sim ev_0\eta\tau_1^2/(\varepsilon_\omega\tau_{ee})$.

To calculate the pure valley current caused by electron-electron scattering we solve the kinetic Eq. (6) with the linearized collision integral

$$\text{St}^{(\text{ee})} = \frac{4\pi}{\hbar} \sum_{\mathbf{k}, \mathbf{k}', \mathbf{p}', \nu'} |u_{\mathbf{p}-\mathbf{p}'}|^2 \delta_{\mathbf{p}+\mathbf{k}, \mathbf{p}'+\mathbf{k}'} \quad (14)$$

$$\times \left\{ \left[f_{\mathbf{c}\mathbf{p}}^{(\nu)} \delta(\varepsilon_{\mathbf{c}\mathbf{p}}^{(\nu)} + \varepsilon_{\mathbf{c}\mathbf{k}}^{(\nu')} - \varepsilon_{\mathbf{c}\mathbf{p}'}^{(\nu)} - \varepsilon_{\mathbf{v}\mathbf{k}'}^{(\nu')}) - (\mathbf{p} \leftrightarrow \mathbf{p}') \right] \right.$$

$$\left. + \left[f_{\mathbf{c}\mathbf{k}'}^{(\nu')} \delta(\varepsilon_{\mathbf{c}\mathbf{p}}^{(\nu)} + \varepsilon_{\mathbf{c}\mathbf{k}}^{(\nu')} - \varepsilon_{\mathbf{v}\mathbf{p}'}^{(\nu)} - \varepsilon_{\mathbf{c}\mathbf{k}'}^{(\nu')}) + (\mathbf{k} \leftrightarrow \mathbf{k}') \right] \right\},$$

where $u_{\mathbf{q}} = 2\pi\hbar\epsilon^2/(\epsilon^*q)$ is the Fourier component of the Coulomb potential and the factor 4 accounts for the spin degeneracy. In Eq. (14), we assume that the warping is small and take it into account only in the arguments of δ -functions. The consequent simplification of $\text{St}^{(\text{ee})}$ consists in summing over the almost collinear momenta. Kinetic Eq. (6) with the simplified electron-impurity collision term $-f_{\mathbf{c}\mathbf{p}}^{(\nu)}/\tau$ takes the form

$$g_{\mathbf{c}\mathbf{p}} = -\frac{\pi e^4}{\hbar^3 v_0 \epsilon^{*2} p} \left[\int_p^\infty dk \left(\sqrt{k} - \sqrt{p} \right)^2 \left(f_{\mathbf{c}\mathbf{k}}^{(+)} + f_{\mathbf{c}\mathbf{k}}^{(-)} \right) \right] \quad (15)$$

$$+ \theta(-\nu \cos 3\varphi_{\mathbf{p}}) \left(\int_p^\infty dk \frac{\sqrt{kp}}{2} f_{\mathbf{c}\mathbf{k}}^{(\nu)} - \frac{p^2}{3} f_{\mathbf{c}\mathbf{p}}^{(\nu)} \right) + \frac{f_{\mathbf{c}\mathbf{p}}^{(\nu)}}{\tau},$$

where $\varphi_{\mathbf{k}} = \varphi_{\mathbf{p}}$ and $\theta(x)$ is the Heaviside step function. In the case of $1/\tau(\varepsilon) = 2\pi^2 e^4 N_i / (\hbar \epsilon^{*2} \varepsilon)$, which corresponds to the momentum relaxation time of electrons due to scattering by Coulomb impurities with the surface density N_i , Eq. (15) can be transformed into a differential equation

$$\gamma u(u^4 + 6\gamma)J''''(u) + \gamma(5u^4 - 16\gamma)J'''(u) + 2u^2(u^4 + 12\gamma)J'(u) + 12u(u^4 - 2\gamma)J(u) = 0 \quad (16)$$

for the function

$$J(u) = \frac{\varepsilon_\omega^2 \int_0^{2\pi} f_{\mathbf{c}\mathbf{p}}^{(+)} \theta(\cos 3\varphi_{\mathbf{p}}) \cos \varphi_{\mathbf{p}} d\varphi_{\mathbf{p}}}{2\pi^2 v_0^2 \tau(\varepsilon_\omega) \sum_{\mathbf{p}} g_{\mathbf{c}\mathbf{p}} \theta(\cos 3\varphi_{\mathbf{p}}) \cos \varphi_{\mathbf{p}}} - \delta(u-1).$$

Here $u = \sqrt{v_0 p / \varepsilon_\omega}$, $J'(u) = dJ(u)/du$, and the parameter $\gamma = \pi N_i \hbar^2 v_0^2 / \varepsilon_\omega^2$ characterizes the rate of electron

scattering by impurities with respect to the electron-electron scattering rate. $J(u)$ satisfies the boundary conditions: $J(1) = J'(1) = 0$, $J''(1) = 2(1+12\gamma)/[\gamma(1+6\gamma)]$, and $J'''(1) = -36/(1+6\gamma)^2$. Finally, the contribution to the valley current induced by electron-electron scattering is given by Eq. (1) with

$$\chi^{(\text{ee})} = -\frac{ev_0\eta\tau(\varepsilon_\omega)t_0^2}{4\pi\varepsilon_\omega} F(\gamma), \quad (17)$$

where $F(\gamma) = \int_0^1 J(u)u^3 du - \gamma J(0)/2 + 1$. The function $F(\gamma)$ determines also the excitation spectrum of valley current since $\gamma \propto 1/\omega^2$. $F(\gamma)$ calculated numerically from Eq. (16) is shown in Fig. 2. The estimation for $\hbar\omega = 1$ eV and $N_i = 10^{12} \text{ cm}^{-2}$ yields $\gamma \sim 10^{-2}$ and $\chi^{(\text{ee})}$ being two orders of magnitude larger than $\chi^{(\text{vel})}$. Thus, for graphene on a substrate with high susceptibility, the mechanism of valley current formation caused by electron-electron scattering dominates.

To summarize, we have shown that the homogeneous excitation of graphene with a linearly polarized light results in a pure valley current and developed the microscopic theory of this effect. Pure valley current is accompanied by no net charge current, but leads to accumulation of valley-polarized carriers at edges of the sample. The valley polarization breaks the time inversion symmetry and also implies the local lowering of space symmetry to the D_{3h} group of a single valley, which lacks the space inversion. The space symmetry lowering can be detected by optical means, e.g., by a second harmonic generation of the probe beam. Another possibility to register the valley current is to convert it into an electric current, which can be realized in curved graphene. The curvature of the graphene sheet produces effective out-of-plane magnetic fields directed oppositely for electrons in the valleys K and K' .¹⁸ Owing to the Lorentz force, the magnetic fields change the directions of partial currents in the valleys giving rise to a measurable net electric current.

We thank E. L. Ivchenko, D. L. Shepelyansky, and A. D. Chepelianskii for stimulating discussions. The work was supported by RFBR, President grant for young scientists, and “Dynasty” Foundation – ICFPM.

¹ A. K. Geim and K. S. Novoselov, The rise of graphene, *Nature Mat.* **6**, 183 (2007).

² A. H. Castro Neto, F. Guinea, N. M. R. Peres, K. S. Novoselov, and A. K. Geim, The electronic properties of graphene, *Rev. Mod. Phys.* **81**, 109 (2009).

³ N. M. R. Peres, The transport properties of graphene: An introduction, *Rev. Mod. Phys.* **82**, 2673 (2010).

⁴ S. A. Tarasenko and E. L. Ivchenko, Pure spin photocurrents in low-dimensional structures, *JETP Lett.* **81**, 231 (2005).

⁵ A. Rycerz, J. Tworzydło, and C. W. J. Beenakker, Valley filter and valley valve in graphene, *Nature Phys.* **3**, 172 (2007).

⁶ J. Karch, S. A. Tarasenko, E. L. Ivchenko, J. Kamann,

- P. Olbrich, M. Utz, Z.D. Kvon, and S.D. Ganichev, Photoexcitation of valley-orbit currents in (111)-oriented silicon metal-oxide-semiconductor field-effect transistors, *Phys. Rev. B* **83**, 121312 (2011).
- ⁷ D. Xiao, W. Yao, and Q. Niu, Valley-contrasting physics in graphene: Magnetic moment and topological transport, *Phys. Rev. Lett.* **99**, 236809 (2007).
- ⁸ D.S.L. Abergel and T. Chakraborty, Generation of valley polarized current in bilayer graphene, *Appl. Phys. Lett.* **95**, 062107 (2009).
- ⁹ T. Oka and H. Aoki, Photovoltaic Hall effect in graphene, *Phys. Rev. B* **79**, 081406 (2009).
- ¹⁰ A.S. Moskalenko and J. Berakdar, Light-induced valley currents and magnetization in graphene rings, *Phys. Rev. B* **80**, 193407 (2009).
- ¹¹ M. V. Entin, L. I. Magarill, and D. L. Shepelyansky, Theory of resonant photon drag in monolayer graphene, *Phys. Rev. B* **81**, 165441 (2010).
- ¹² J. Karch, P. Olbrich, M. Schmalzbauer, C. Zoth, C. Brinsteiner, M. Fehrenbacher, U. Wurstbauer, M.M. Glazov, S. A. Tarasenko, E. L. Ivchenko, D. Weiss, J. Eroms, R. Yakimova, S. Lara-Avila, S. Kubatkin, and S.D. Ganichev, Dynamic Hall effect driven by circularly polarized light in a graphene layer, *Phys. Rev. Lett.* **105**, 227402 (2010).
- ¹³ E. McCann, K. Kechedzhi, V.I. Fal'ko, H. Suzuura, T. Ando, and B.L. Altshuler, Weak-localization magnetoresistance and valley symmetry in graphene, *Phys. Rev. Lett.* **97**, 146805 (2006).
- ¹⁴ D.N. Mirlin, Optical alignment of electron momenta in GaAs-type semiconductors, in *Optical Orientation*, edited by F. Meier and B.P. Zakharchenya (Elsevier Science, Amsterdam, 1984).
- ¹⁵ D.M. Basko, S. Piscanec, and A.C. Ferrari, Electron-electron interactions and doping dependence of the two-phonon Raman intensity in graphene, *Phys. Rev. B* **80**, 165413 (2009).
- ¹⁶ E. G. Mishchenko, Effect of electron-electron interactions on the conductivity of clean graphene, *Phys. Rev. Lett.* **98**, 216801 (2007).
- ¹⁷ D. C. Elias, R. V. Gorbachev, A. S. Mayorov, S. V. Morozov, A. A. Zhukov, P. Blake, K. S. Novoselov, A. K. Geim, and F. Guinea, Dirac cones reshaped by interaction effects in suspended graphene, arXiv:1104.1396.
- ¹⁸ F. Guinea, M. I. Katsnelson, and A. K. Geim, Energy gaps and a zero-field quantum Hall effect in graphene by strain engineering, *Nature Phys.* **6**, 30 (2010).